Annals of Glaciology 37 2003

A mesoscopic approach for modelling texture evolution of polar ice including recrystallization phenomena

GÜNTER GÖDERT
Fakultät Maschinenbau, Lehrstuhl für Mechanik, Universität Dortmund, D-44221 Dortmund, Germany
E-mail: ggoedert@mech.mb.uni-dortmund.de

ABSTRACT. A material model for the simulation of anisotropic behaviour due to texture development in polar ice is presented. Emphasis is laid on the strain-induced texture development and its relaxation due to rotation recrystallization and grain boundary migration in the low-velocity regime. The model is based on two scales (mesoscopic approach). Kinematics, balance equations and constitutive assumptions are defined with respect to the grain level (mesoscale). Slip-system behaviour is assumed to be Newtonian. Recrystallization and grain boundary migration are taken into account via a diffusion-type evolution of the crystallites orientation. Due to the inextensibility of the ice crystallites along their c axes, the Sachs–Reuss assumption is adopted. Volume averaging yields associated macroscopic relations, where the internal structure is represented by a second-order structure tensor. The proposed approach is illustrated by applying it to initially isotropic material under homogeneous deformation, giving results qualitatively in agreement with experimental evidence. Finally, it is shown that the proposed model is, under some simplifying conditions, directly related to phenomenological internal variable models (e.g. Morland and Staroszczyk, 1998).

1. INTRODUCTION

The flow of polar ice masses plays an essential part in climate simulations, i.e. past climate history, at least to some extent stored in ice particles, is expected to be reconstructable by analyzing ice cores (e.g. Thorsteinsson and others, 1997). The impact of the actual orientation distribution of c axes (texture) on thermomechanical (flow) properties is evident from laboratory and field data (e.g. Bouchez and Duval, 1982; Budd and Jacka, 1989). Ice crystals possess hexagonal symmetry with three glide planes (basal, prismatic and pyramidal) where creep deformation occurs mainly along the basal plane, represented by its c axis (Bouchez and Duval, 1982). Several authors have developed constitutive models for (strain-)induced anisotropy capable of taking texture changes into account (e.g. Van der Veen and Whillans, 1994; Castelnau and others, 1996). The common idea is: based on knowledge of the behaviour of crystallites (mesoscale), the macro-scale behaviour is derived via homogenization. However, since the model is to be used for large-scale flow simulations the numerical effort should be as small as possible.

This problem was recently addressed when fabric evolution was considered using tensor-valued internal variables (e.g. Morland and Staroszczyk, 1998). In contrast to this approach, where the number of fields is increased, Gagliardini and Meyssonnier (1999) and Gödert and Hutter (2000) increased the number of field quantities. To this end, the classical space, $\mathbb{R}^n_{\mathbf{x}}$, is extended to $\mathbb{V} = \mathbb{R}^n_{\mathbf{x}} \times \mathbb{S}^d$, where $n = 2, 3$ and $d = 1, 2$. d denotes the dimension of the unit sphere $\mathbb{S}^d$. This implies that the position of a grain as well as its size and shape are considered unimportant. Consequently, there remains the orientation of a grain, here expressed by $\mathbf{n} : \mathbb{S}^d$. $\mathbf{x}$ indicates the macroscopic position of a material point. Direct numerical analysis with respect to the mesoscopic space, $\mathbb{V}$, would require too much effort, so the meso-approach implies the statistical concept of orientation distribution function (ODF), where the ODF, $f_{(\mathbf{n},\mathbf{x},t)} \in L^2_{(\mathbb{S}^d)}$, may be interpreted as a probability density fulfilling

$$\int_{(\mathbb{S}^d)} f_{(\mathbf{n},\mathbf{x},t)} \, \mathrm{d}\mathbb{S}^d = 1 \,. \tag{1}$$

Equation (1) already suggests the rule yielding macroscopic quantities, $\Xi_{(\mathbf{x},t)}$, from those defined on the mesoscopic scale, $\tilde{\Xi}_{(\mathbf{n},\mathbf{x},t)}$,

$$\int_{(\mathbb{S}^d)} \tilde{\Xi}_{(\mathbf{n},\mathbf{x},t)} f_{(\mathbf{n},\mathbf{x},t)} \, \mathrm{d}\mathbb{S}^2 = \Xi_{(\mathbf{x},t)} = \left\langle \tilde{\Xi}_{(\mathbf{n},\mathbf{x},t)} \right\rangle . \tag{2}$$

The above considerations can be derived more descriptively if one assumes a *volume of influence*, v, around each material point $\mathbf{x}$ of the continuum. Considering that the deformation is incompressible, macroscopic entities can be obtained simply by volume averaging. Then f is given as the volume fraction of $v_{\mathbf{n}}$ and v, where $v_{\mathbf{n}}$ represents the volume of equally oriented crystallites within v, so that $vf = v_{\mathbf{n}}$. Note that all quantities associated with the grain level are denoted by the subindex $()_{\mathbf{n}}$, whereas, if it seems necessary to prevent misunderstandings, the macroscopic or polycrystal level is indicated by $()_{\mathbf{a}}$ (see Appendix C for further explanation of the underlying notation). Applying Equation (2) to the mesoscopic structure, one obtains the associated macroscopic structure tensors as

$$\overset{\langle k \rangle}{\mathbf{A}} = \left\langle \overset{\langle k \rangle}{\mathbf{N}} \right\rangle . \tag{3}$$

https://doi.org/10.3189/172756403781815375 Published online by Cambridge University Press

2. KINEMATICS

Ice single crystallites are treated as "rigidly elastic" viscous material. In general, for hexagonal crystals the contribution of pyramidal slip can be neglected. Furthermore, reorientation of the c axes is then governed solely by basal slip, so that, since we are interested in the evolution of the c axes, for the sake of conciseness we may restrict the following to basal slip only. Then decomposition of the deformation gradient into an "elastic" rotation, $\mathbf{R_n}$, and an inelastic deformation, $\mathbf{F}^{\mathrm{I}}_{\mathbf{n}} = \mathbf{I} + \gamma \mathbf{e}_\gamma \otimes \mathbf{n}$, leads to

$$\mathbf{F_n} = \mathbf{R_n}\mathbf{F}^{\mathrm{I}}_{\mathbf{n}} \quad \text{and} \quad \dot{\mathbf{F}}_{\mathbf{n}}\mathbf{F}^{-1}_{\mathbf{n}} = \mathbf{L_n} = \mathbf{D_n} + \mathbf{W_n}\,, \tag{4}$$

the mesoscopic deformation and its associated velocity gradient, respectively. Here, the overdot indicates time differentiation, and γ and $\mathbf{e}_\gamma$ denote the amount of basal slip and its direction, respectively. Here, $\mathbf{D_n} = \mathrm{sym}(\mathbf{L_n})$ denotes the stretching, and $\mathbf{W_n} = \mathrm{skw}(\mathbf{L_n})$ the spin. Further additive decomposition of the total grain spin $\mathbf{W_n}$ into its elastic and inelastic contributions,

$$\mathbf{W_n} = \mathbf{W}^{\mathrm{E}}_{\mathbf{n}} + \mathbf{W}^{\mathrm{I}}_{\mathbf{n}}\,, \tag{5}$$

may be obtained by straightforward calculation, whereas stretching is completely inelastic, $\mathbf{D_n} = \mathbf{D}^{\mathrm{I}}_{\mathbf{n}}$. Due to the inextensibility of c axes, their evolution is given via the "elastic" spin, $\mathbf{W}^{\mathrm{E}}\mathbf{n} = \dot{\mathbf{n}}$ (e.g. Dafalias, 1984), yielding

$$\dot{\mathbf{n}} = (\mathbf{W_n} - \mathbf{W}^{\mathrm{I}}_{\mathbf{n}}) \cdot \mathbf{n}\,, \tag{6}$$

where the inelastic spin, $\mathbf{W}^{\mathrm{I}}_{\mathbf{n}}$, can be expressed in terms of the inelastic mesoscale stretching, $\mathbf{D_n}$,

$$\mathbf{W}^{\mathrm{I}}_{\mathbf{n}} = \mathbf{D_n}\mathbf{N} - \mathbf{N}\mathbf{D_n}\,. \tag{7}$$

3. BALANCE EQUATIONS

Let $\mathbf{z} = \mathbf{x} + \mathbf{n}$ describe a point of $\tilde{\Omega} = \Omega_{\mathbf{x}} \oplus \Omega_{\mathbf{n}}$, an open domain of the extended space $\mathtt{V}$, where $\mathbf{x} : \Omega_{\mathbf{x}} \subset \mathbb{R}^{\mathtt{n}}_{\mathbf{x}}$ and $\mathbf{n} : \Omega_{\mathbf{n}} \subset \mathtt{S}^{\mathtt{d}}$, with $n \geq d$, $n \in \{2, 3\}$ and $d \in \{1, 2\}$. If Ψ denotes the density of a physical quantity, it globally changes its value through production and external supply, π_Ψ, as well as by flux, $\mathbf{q}_\Psi$. Straightforward generalization of Reynolds' transport theorem gives

$$\frac{\mathrm{d}}{\mathrm{d}t}\int\limits_{\tilde{\Omega}} \Psi \,\mathrm{d}v = \int\limits_{\tilde{\Omega}} \left[\frac{\partial \Psi}{\partial t} + \nabla_{\mathbf{z}} \cdot (\mathbf{v_z}\Psi)\right] \mathrm{d}v\,, \tag{8}$$

where the gradient, $\nabla_{\mathbf{z}} = \nabla_{\mathbf{x}} + \nabla_{\mathbf{n}}$, as well as velocity, $\mathbf{v_z} = \mathbf{v_x} + \mathbf{v_n}$, and flux, $\mathbf{q}_\Psi = \mathbf{q}_{\Psi_{\mathbf{x}}} + \mathbf{q}_{\Psi_{\mathbf{n}}}$, can be decomposed, leading to the generalized balance

$$\frac{\partial \Psi}{\partial t} + \nabla_{\mathbf{x}} \cdot (\mathbf{v_x}\Psi - \mathbf{q}_{\Psi_{\mathbf{x}}}) + \nabla_{\mathbf{n}} \cdot (\mathbf{v_n}\Psi - \mathbf{q}_{\Psi_{\mathbf{n}}}) = \pi_\Psi\,. \tag{9}$$

Without considering the details, the (pure mechanical) problem will be reduced to a set of balance equations consisting of the macroscopic balances of mass, momentum and angular momentum supplemented by the mesoscopic balance of orientation (Equation (10)). From Equation (9), the mass balance is obtained if the mesoscopic mass density $\Psi = v_{\mathbf{n}} = vf$ is substituted. Independency of f and v then requires the macroscopic mass balance, $\partial_t v + \nabla_{\mathbf{x}} \cdot (\mathbf{v_x} v) = 0$, as well as the mesoscopic mass balance,

$$\partial_t f + \mathbf{v_x} \cdot \nabla_{\mathbf{x}} f + \nabla_{\mathbf{n}} \cdot (\mathbf{v_n} f + \mathbf{q}_{v_{\mathbf{n}}}) = 0\,, \tag{10}$$

which describes the evolution of the orientation distribution. Supplemented by an appropriate initial condition, Equation (10) can be solved for f if $\mathbf{v_n}$ and $\mathbf{q}_{v_{\mathbf{n}}}$ are given.

4. CONSTITUTIVE ASSUMPTIONS

The constitutive equations are formulated in two steps. First the behaviour of an isolated crystallite is described as a function of the set of macroscopic variables, $S = \{\mathbf{X}, \mathbf{A}\}$, where $\mathbf{X} = \mathbf{X}^T$ represents a generalized external driving force. In a second step, the interaction of the single crystallites within their polycrystalline environment is taken into account. Let $\tilde{\Psi}_{\mathbf{n}}$ and $\Psi_{\mathbf{n}}$ denote an additive quantity of an isolated and an embedded crystallite, respectively, then a consistent description is defined by

$$\Psi_{\mathbf{n}} = \alpha_\Psi \Psi_{\mathbf{a}} + (1 - \alpha_\Psi)\tilde{\Psi}_{\mathbf{n}}\,, \tag{11}$$

where α_Ψ represents a function of macroscopic variables only (e.g. Gödert, 1999). The limit cases of a random and a completely aligned c-axes distribution are governed by $\alpha_\Psi \to 0$ and $\alpha_\Psi \to 1$, respectively. Note that, due to $\Psi_{\mathbf{a}} = \langle \tilde{\Psi}_{\mathbf{n}} \rangle$, consistency is fulfilled by construction, i.e. the macroscopic behaviour of the material is invariant with respect to the α_Ψ modification. That is, a material quantity is properly defined by α_Ψ and $\tilde{\Psi}_{\mathbf{n}}$.

The set of mesoscopic variables to be determined via constitutive assumptions then comprises the total spin $\tilde{\mathbf{W}}_{\mathbf{n}}$, the stretching $\tilde{\mathbf{D}}_{\mathbf{n}}$ as well as the Cauchy stress $\tilde{\mathbf{T}}_{\mathbf{n}}$, the orientation flux vector $\tilde{\mathbf{q}}_{v_{\mathbf{n}}}$ and in the second step the corresponding weighting coefficients α_W, α_D, α_T and α_q, respectively.

4.1. Isolated single crystal

Intracrystalline slip

Due to the lack of five independent slip systems the Sachs–Reuss or static assumption is adopted. Furthermore the Voigt–Taylor assumption is applied for the spin, yielding

$$\tilde{\mathbf{T}}_{\mathbf{n}} = \mathbf{T} \qquad \text{and} \qquad \tilde{\mathbf{W}}_{\mathbf{n}} = \mathbf{W}\,. \tag{12}$$

According to related work, slip is assumed to be well approximated by Newtonian creep. Anisotropy of the single crystal is determined by its c axis, yielding a transversely isotropic material behaviour compactly written as

$$\tilde{\mathbf{D}}_{\mathbf{n}} = \frac{\mu}{2}\mathcal{C}_{\mathbf{n}} \cdot\cdot\, \mathbf{T}\,, \tag{13}$$

where $\mathcal{C}_{\mathbf{n}} = [2(1-\beta)\mathcal{P}_{\mathbf{n}} + \beta\mathcal{I}_{\mathrm{dev}}]$. $\mathcal{P}_{\mathbf{n}} = \mathcal{I}_{\mathrm{sym}} \cdot \mathbf{N} \cdot\cdot\, \mathcal{I}_{\mathrm{sym}} - \mathcal{N}$, and μ denotes the basal fluidity. This form is equivalent to the expression proposed by Gagliardini and Meyssonnier (1999), but in practice the grain anisotropy parameter $\beta \ll 1$.

Rotation recrystallization (polygonization)

Rotation recrystallization or polygonization is generally associated with the formation of (sub)grain boundaries due to heterogeneous loading. This fragmentation process mainly affects grains that are not well oriented for dislocation glide, so-called "hard grains". Since fragmentation is accompanied by specific reorientation of certain lattice portions, the resulting subgrains tend to be softer than their parent grains (e.g. Poirier, 1985). From a mathematical point of view, orientation moves from hard to soft configurations. There is a similarity between heat flux and what we call orientation flux. Analogous to heat-flux problems, rotation recrystallization can be considered as a diffusive flux of orientation described via Fick's law with respect to the hardness, $\mathbf{q}_{v_{\mathbf{n}}} = -\lambda_{\mathbf{n}} \nabla_{\mathbf{n}}(H_n)$. On the other hand, considering that, for each orientation, only a certain fraction of grains polygonizes, fragmentation may also be understood in the sense of Brownian motion. Hardness, $\lambda_H H_n > 0$, represents then an external loading and can therefore be expected as a

https://doi.org/10.3189/172756403781815375 Published online by Cambridge University Press

general function of $\mathbf{N}$ and $\mathbf{X}$, where $\lambda_H \geq 0$ is assumed to depend on macroscopic quantities only. Yet experience tells us that direct (normal) loading with respect to the basal plane is most important, so the set of independent variables can be reduced to the invariants $I_{\mathbf{NX}^i} = (\mathbf{N}, \mathbf{X}^i)$ $(i = 1, 2, 3)$. Furthermore, restricting non-linearity of H_n to quadratic order, it is supposed to be appropriately represented by

$$\tilde{H}_{\mathbf{n}} = \sum_{(i=1,2)} h_i I_{\mathbf{NX}^i}^{3-i}\,, \tag{14}$$

where the coefficients h_i are isotropic functions of the set S.

Grain boundary migration

If grain growth takes place, nearest neighbours are always involved. Therefore, grain growth is in general "intra-orientational", not describable by diffusion-type evolutionary terms (but rather by an appropriate production term). Montagnat and Duval (2000) developed a model for the dislocation balance at the low-velocity regime of grain boundary migration, which is essentially based on the hypothesis that grain boundary migration and polygonization are concurrent processes (Montagnat and Duval, 2000). Subgrains created by polygonization are supposed to merge again, so that the (mean) orientation of the grain remains the same during this circular process. However, neither the orientation of subgrains nor that of neighbouring grains was explicitly taken into account. It seems to be a reasonable working hypothesis that a grain grows at the expense of its neighbours, whatever its orientation. Grain boundary migration, at least in the low-velocity regime, can then be modelled by an evolutionary term similar to that derived for rotation recrystallization, but acting in the "opposite direction".

4.2. Embedded single crystal

Considering Equations (12), the coefficients α_W and α_T are already defined. α_D can be motivated by alternative (second-order) kinematically compatible deformation mechanisms like dislocation climb and rotation recrystallization, yielding

$$\mathbf{D}_{\mathbf{n}} = \alpha_D \mathbf{D} + (1 - \alpha_D)\tilde{\mathbf{D}}_{\mathbf{n}}\,, \tag{15}$$

where α_D is a monotonic function of the degree of alignment, α_P, defined below. Recalling that $\alpha_D \to 1$ for completely aligned c axes, a distinction between meso- and macro-scale becomes obsolete, leading to the consistent result $\mathbf{D}_{\mathbf{n}} = \mathbf{D}$. Furthermore, the physically obligatory energy-consistency condition $\mathbf{T} \cdot\cdot\, \mathbf{D} = \langle \mathbf{T}_{\mathbf{n}} \cdot\cdot\, \mathbf{D}_{\mathbf{n}} \rangle$ is fulfilled. The hardness of an embedded grain is formally given by $H_{\mathbf{n}} = \alpha_H H_{\mathbf{a}} + (1 - \alpha_H)\tilde{H}_{\mathbf{n}}$, where α_H again denotes a function of the degree of c-axes alignment. However, considering that instead of the hardness its gradient, $\nabla_{\mathbf{n}}\tilde{H}_{\mathbf{n}}$, represents the constitutive quantity, the term $H_{\mathbf{a}}$ becomes meaningless. Then the orientation flux is given by

$$\mathbf{q}_{v_n} = -\lambda_{\mathbf{n}} \nabla_{\mathbf{n}} \tilde{H}_{\mathbf{n}} \tag{16}$$

($\lambda_{\mathbf{n}}$ comprises $(1 - \alpha_H)$). In order to describe the intensity of the orientation flux, we suggest that the misorientation angle between polygonized grains depends linearly on the number of dislocations suggesting $\lambda_{\mathbf{n}} \approx n_d \lambda_{\mathbf{a}}$. Assuming further the same dislocation density ρ_d for all equal orientated grains, one may conclude from $n_d = \rho_d v_{\mathbf{n}} \approx f$ the relocation

$$\lambda_{\mathbf{n}} = f \lambda_{\mathbf{a}}\,. \tag{17}$$

Rotation recrystallization (as well as grain boundary migration) then becomes describable via

$$\mathbf{q}_{v_n} = -\lambda_{\mathbf{n}} \nabla_{\mathbf{n}} \tilde{H}_{\mathbf{n}}\,. \tag{18}$$

4.3. Homogenization

Macroscopic quantities are obtained by applying Equation (2), yielding identities for the stress and the spin. Recalling the invariance of the α modification with respect to the macroscopic behaviour, the strain-rate tensor is given as

$$\mathbf{D} = \frac{\mu}{2} \mathcal{C}_{\mathbf{a}} \cdot\cdot\, \mathbf{T}, \qquad \mathcal{C}_{\mathbf{a}} = \langle \mathcal{C}_{\mathbf{n}} \rangle\,. \tag{19}$$

Hence, Equation (19) is completely determined if the temporal evolution of the fourth-order structure tensor $\mathcal{A}$ is known. Referring to related work, the following considerations will be restricted to orthotropic material behaviour, i.e. to the evolution of the second-order tensor. Taking the mesoscopic mass balance (Equation (10)) into account, the local change of the structure is given as

$$\partial_{\mathbf{t}} \mathbf{A} = 2\,\mathrm{sym}(\langle \dot{\mathbf{n}} \otimes \mathbf{n} \rangle) - \left\langle f^{-1} \nabla_{\mathbf{n}} \cdot \mathbf{q}_{v_n} \mathbf{N} \right\rangle. \tag{20}$$

Applying Equations (6), (7) and (15) and considering $2\mathcal{P}_{\mathbf{n}} \cdot\cdot\, \mathcal{P}_{\mathbf{n}} = \mathcal{P}_{\mathbf{n}}$, the Jaumann rate $\overset{\circ}{\mathbf{A}} = \partial_{\mathbf{t}} \mathbf{A} - 2\,\mathrm{sym}(\mathbf{WA})$ takes the form

$$\overset{\circ}{\mathbf{A}} = -\mathcal{P}_{\mathbf{a}} \cdot\cdot \left(2\alpha_D \mathbf{D} + \frac{\mu(1 - \alpha_D)}{2} \mathbf{T} \right) + \left\langle f^{-1} \nabla_{\mathbf{n}} \cdot \mathbf{q}_{v_n} \mathbf{N} \right\rangle. \tag{21}$$

Making use of Equations (19), (17) and (18) with $\nabla_{\mathbf{n}} \tilde{H}_{\mathbf{n}} = h_i (3 - i)\, I_{\mathbf{NX}^i}^{2-i} \nabla_{\mathbf{n}} I_{\mathbf{NX}^i}$, $\mathbf{q}_{v_n} \cdot \mathbf{n} = 0$ and application of Gauss theorem (on the unit sphere (e.g. Appendices A and B)), the co-rotational evolution of $\mathbf{A}$ (Equation (21)) takes the form

$$\begin{aligned} \overset{\circ}{\mathbf{A}} = &- \left[(1 - \alpha_D) \mathcal{P}_{\mathbf{a}} \cdot\cdot\, \mathcal{C}_{\mathbf{a}}^{-1} + 2\alpha_D \mathcal{P}_{\mathbf{a}} \right] \cdot\cdot\, \mathbf{D} \\ &- \lambda_{\mathbf{a}} \sum_{(i)} \left\langle \mathcal{P}_{\mathbf{n}} \cdot\cdot\, \mathbf{X}^i (3 - i) h_i I_{\mathbf{NX}}^{2-i} \right\rangle. \end{aligned} \tag{22}$$

4.4. Closure approximation

The mean projection operator, $\mathcal{P}_{\mathbf{a}}$, contains the fourth-order structure tensor, so the second-order evolution equation (21) is not closed. The same argument holds for the fourth-order evolution equation; here the sixth-order structure tensor is needed. Generally the evolution of the $2n$th moment necessitates the $2(n+1)$th moment, resulting in an infinite hierarchy of equations. Since we restricted considerations to orthotropic material behaviour, it suffices to describe the evolution of the second-order structure tensor. Hence, an appropriate expression for $\mathcal{A}$ is needed. To this end, Gagliardini and Meyssonnier (1999) and Gödert and Hutter (2000) restricted the ODF by certain symmetry conditions (to orthotropy), so that explicit computation of $\mathcal{A}$ becomes feasible under plane flow conditions. In contrast to those restrictions, we use a closure approximation, so the model is not restricted to plane flow. Recalling that c-axes rearrangement takes place monotonically, in the sense that fabric develops continuously from randomly distributed c axes at the top of an ice sheet to more-or-less completely aligned c axes at its bottom, an appropriate approximation of the fourth-order terms must bridge the gap between the two extremal distributions. In accordance with Advani and Tucker (1987), this is achieved by approximating $\mathcal{P}_{\mathbf{a}}$ by the so-called hybrid closure

$$\mathcal{P}_{\mathbf{a}} = (1 - \alpha_P) \mathcal{P}_{\mathbf{a}}|_{\mathrm{random}} + \alpha_P \mathcal{P}_{\mathbf{a}}|_{\mathrm{aligned}}\,, \tag{23}$$

https://doi.org/10.3189/172756403781815375 Published online by Cambridge University Press

where

$$\mathcal{P}_{\mathbf{a}}|_{\text{aligned}} = \left(\mathcal{I}_{\text{sym}} \cdot \mathbf{A} \cdot\cdot \mathcal{I}_{\text{sym}} - \mathbf{A} \otimes \mathbf{A}\right),$$

$$\mathcal{P}_{\mathbf{a}}|_{\text{random}} = \frac{1}{5}\mathcal{I}_{\text{dev}},$$

and

$$2\alpha_P = (3I_{\mathbf{A}^2} - 1) \tag{24}$$

denotes the degree of alignment for the case $n = 3$ and $d = 2$.

5. APPLICATION

To carry out a completely coupled analysis, Equation (22) is to be substituted into

$$\dot{\mathbf{A}} = \partial_t \mathbf{A} + \mathbf{v}_{\mathbf{x}} \cdot \nabla_{\mathbf{x}} \mathbf{A}. \tag{25}$$

Alternatively, with a view to efficient numerical considerations, the local time derivative can be split into a material and a spatial part, $\partial_{\mathbf{t}}() = \partial_{\tau_1}() + \partial_{\tau_2}()$, yielding

$$\dot{\mathbf{A}} = \partial_{\tau_1} \mathbf{A}, \quad 0 = \partial_{\tau_2} \mathbf{A} + \mathbf{v}_{\mathbf{x}} \cdot \nabla_{\mathbf{x}} \mathbf{A}. \tag{26}$$

Accordingly, the evolution of $\mathbf{A}$ is decoupled into a pure material and spatial part (e.g. Equations $(26)_{\text{a}}$ and $(26)_{\text{b}}$). The constitutive model is then completely given by Equations (19), (22) and (26) or (25). It will be shown that besides the non-diffusive, i.e. $\mathbf{q}_{v_n} = 0$, static models of Gagliardini and Meyssonnier (1999), i.e. $\alpha_D = 0$, and Gödert (1999), i.e. $\beta = 0$, the diffusive model of Staroszczyk and Morland (2001) can also to some extent be treated as a special case within the presented approach.

In the following, several special cases will be taken into account for the material part of Equation (26). First, uniaxial, compressive loading is considered. Here a single-maximum fabric develops along the loading axis, which at the same time represents the direction of maximum hardness. H_n may therefore be qualitatively identified with the ODF. Applying $\mathbf{q}_{v_{\mathbf{n}}} = -\lambda_{\text{A}} \nabla_{\mathbf{n}}(f)$, with $\lambda_{\text{A}} = \text{const.}$, the second righthand term of Equation (21) takes the form

$$\langle f^{-1} \nabla_{\mathbf{n}} \cdot \mathbf{q}_{v_{\mathbf{n}}} \mathbf{N} \rangle = \lambda_{\text{A}} (\mathbf{I} - 3\mathbf{A}). \tag{27}$$

The local evolution of the structure tensor is then given as

$$\overset{\circ}{\mathbf{A}} = -\left[(1 - \alpha_D)\mathcal{P}_{\mathbf{a}} \cdot\cdot\, \mathcal{C}_{\mathbf{a}}^{-1} + 2\alpha_D \mathcal{P}_{\mathbf{a}}\right] \cdot\cdot\, \mathbf{D} + \lambda_{\text{A}} (\mathbf{I} - 3\mathbf{A}). \tag{28}$$

In general, λ_{A} is a function of the ODF (e.g. Equation (17)), so the resulting relaxation (Equation (27)) is more likely related to dynamic recrystallization (rapid grain boundary) than to the deletion of preferably orientated subgrain boundaries.

General loading

For the sake of simplicity, we assume $\beta = 0$ for the evolution equation. Furthermore, the diffusive term is restricted to depend linearly on the loading, but remains invariant under a change in loading direction. These requirements are met if $i = 2$ and $h = h(I_{\mathbf{A}^2}) I_{\mathbf{D}^2}^{-0.5}$, yielding

$$2\,\text{sym}(\langle f^{-1} \mathbf{q}_{v_{\mathbf{n}}} \otimes \mathbf{n} \rangle) = 4\lambda_{\text{B}} \mathcal{P}_{\mathbf{a}} \cdot\cdot\, \overline{\mathbf{D}}, \tag{29}$$

where, with $\overline{\mathbf{D}} = \mathbf{D}^2 / \sqrt{\mathbf{D} \cdot\cdot \mathbf{D}}$ and $\lambda_{\text{B}} = \text{const.}$, the co-rotational evolution can be written as

$$\overset{\circ}{\mathbf{A}} = -[2\alpha_D \mathcal{P}_{\mathbf{a}} + (1 - \alpha_D)\mathcal{I}_{\text{dev}}] \cdot\cdot\, \mathbf{D} - \lambda_{\text{B}} \mathcal{P}_{\mathbf{a}} \cdot\cdot\, \overline{\mathbf{D}}. \tag{30}$$

Non-diffusive, coaxial loading

First, we consider pure mechanical texture evolution, i.e. $\lambda_{\text{A}} = 0$. Then due to coaxial loading, i.e. $\mathbf{W} = 0$, Equation $(26)_{\text{a}}$ reduces to

$$\overset{\circ}{\mathbf{A}} = -\mathbf{D} \tag{31}$$

if the above model is restricted to basal glide only, that is $\alpha_D = 0$ as well as $\beta = 0$. Integration of Equation (31), $\mathbf{A} = \mathbf{A}_0 + \int \overset{\circ}{\mathbf{A}}\, \mathrm{d}t$, carried out via exponential mapping of the actual deformation gradient, $\mathbf{F}_k = \exp(\mathbf{L}_k \delta t)\mathbf{F}_{k-1}$, reveals that the second-order structure tensor $\mathbf{A}$ can be replaced by the Cauchy–Green tensor $\mathbf{B}$ recursively defined by $\mathbf{B}_k = \exp(\mathbf{L}_k \delta t)\mathbf{B}_{k-1} \exp(\mathbf{L}_k^T \delta t)$, so that, if $\mathbf{B}_0 = \mathbf{I}$, one obtains the relation

$$\mathbf{B}_{(t)} = \exp\left(\int_{t_0}^{t} \mathbf{L}\, \mathrm{d}t\right) \exp\left(\int_{t_0}^{t} \mathbf{L}^T\, \mathrm{d}t\right) = \exp\left(2 \int_{t_0}^{t} \mathbf{D}\, \mathrm{d}t\right). \tag{32}$$

Starting from a random c-axes distribution, $\mathbf{A}_0 = \frac{1}{3}\mathbf{I}$, the actual structure tensor is given by

$$\mathbf{A} = \frac{1}{3}\mathbf{I} + \ln \sqrt{\mathbf{B}^{-1}} = \frac{1}{3}\mathbf{I} - \mathbf{H}, \tag{33}$$

where $\mathbf{H}$ represents the Hencky strain tensor. Although this holds true only for path-independent problems, one might be in favour of taking $\mathbf{H}$ or equivalently $\mathbf{B}$ as the general macroscopic structural variable. With this in mind and in order to accomplish the evolution equation, the spatial part (Equation $(26)_{\text{b}}$) can be written in terms of the deformation gradient, $\mathbf{F}$, so that further mesoscopic considerations become obsolete:

$$\partial_t \mathbf{F} + \mathbf{v}_{\mathbf{x}} \cdot \nabla_{\mathbf{x}}(\mathbf{F}) = 0. \tag{34}$$

In principle, this is what Morland and Staroszczyk (1998) proposed ad hoc, when they assumed the deviatoric stress to be an isotropic function of the eigenvectors and eigenvalues of $\mathbf{B}$. Staroszczyk and Morland (2001) extended their model to migration recrystallization by adding a term proportional to $(\mathbf{I} - 3\mathbf{B})$, which also agrees with our perceptions, if $\mathbf{A}$ is replaced by $\mathbf{B}$ in Equation (27). This shows that, with respect to the evolution of the internal structure, their model is closely related to the proposed static, single-slip model (i.e. basal glide only), with $\alpha_D = 0$, $\beta = 0$.

Simple shear

In order to assess the capabilities of the model, a simple shear deformation, $\mathbf{D} = \dot{\kappa}\,\text{sym}(\mathbf{e}_1 \otimes \mathbf{e}_2)$, is taken into account. Two parameter variations of the evolution equation are considered, whereas the stress–strain-rate relation for both cases is based on $\beta = 0.25$ and $\alpha = 1.2$, where the interaction parameter α, defined via

$$\alpha_D = \alpha \alpha_P, \tag{35}$$

is determined from comparison with field data (e.g. Gödert, 1999). The grain anisotropy parameter $\beta = 0.25$ is taken from Gagliardini and Meyssonnier (1999) as a reasonable choice in view of the resulting c-axes distribution. First, diffusive as well as grain interaction processes are neglected completely, i.e. $H_{\mathbf{n}} = \text{const.}$ and $\alpha = 0$, respectively. Hence, (double slip) model A coincides with the constitutive equations of Gagliardini and Meyssonnier (1999). Model B (single slip),

https://doi.org/10.3189/172756403781815375 Published online by Cambridge University Press

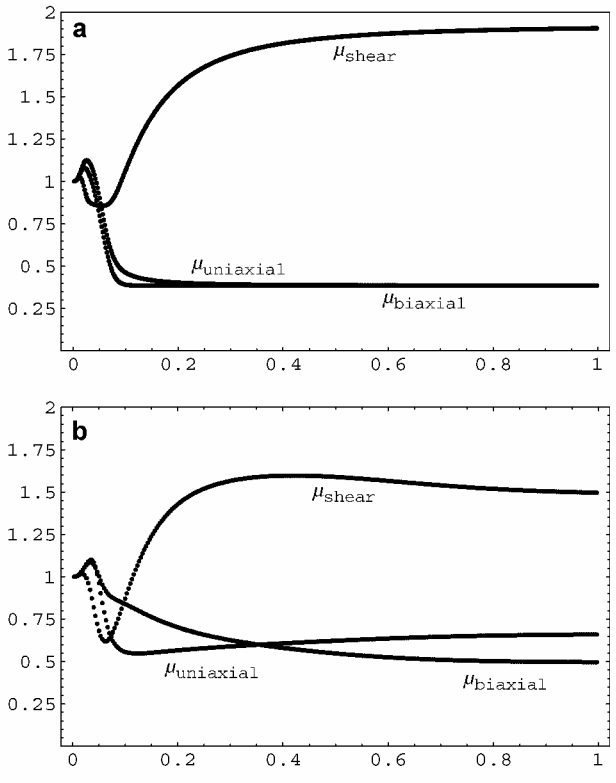

Fig. 1. Evolution of the normalized shear, uniaxial- and biaxial-compressive fluidities (μ_{shear}, $\mu_{uniaxial}$, $\mu_{biaxial}$) due to normalized simple shear deformation: (a) model A ($\alpha = 0.0$, $\beta = 0.25$); (b) model B ($\alpha = 1.2$, $\beta = 0.0$).

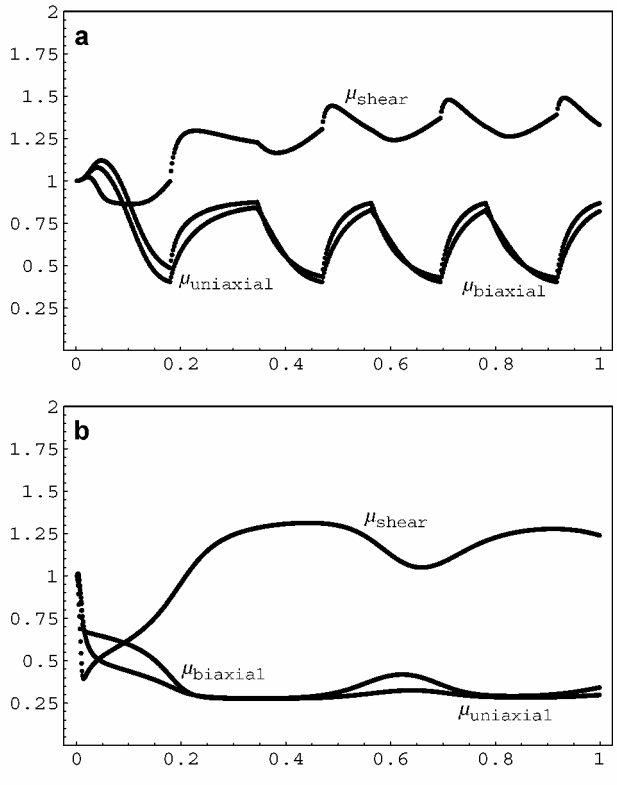

Fig. 2. Same as Figure 1, but with model A ($\alpha = 0.0$, $\beta = 0.25$) plus λ_A-type (a) and λ_B-type diffusion (b) controlled through the degree of alignment, α_P.

the second variation, is chosen in accordance with Gödert (1999), i.e. $\alpha = 1.2$.

Model A (Fig. 1a): $\alpha = 0.0, \quad \beta = 0.25,$

$$\overset{\circ}{\mathbf{A}} = -2\left[\beta \mathcal{P}_{\mathbf{a}}{}^{-1} + 2(1-\beta)\mathcal{I}_{\mathrm{dev}}\right]^{-1} \cdot\cdot\, \mathbf{D} \qquad (36)$$

Model B (Fig. 1b): $\alpha = 1.2, \quad \beta = 0.0,$

$$\overset{\circ}{\mathbf{A}} = -\left[2\alpha_D \mathcal{P}_{\mathbf{a}} + (1-\alpha_D)\mathcal{I}_{\mathrm{dev}}\right] \cdot\cdot\, \mathbf{D} \qquad (37)$$

Diffusive effects, representing the wide range of possible material responses, are principally reflected in Figure 2 denoting the fluidities if rearrangement of the orientations occurs due to rotation recrystallization. In accordance with the above considerations, diffusion is implemented via Equations (27) and (30), in the following called λ_A- and λ_B-type diffusion, respectively. As one would expect, $\lambda_A = \text{const.}$ can be used to adjust the value of the maximum alignment (not plotted here). In contrast, λ_B-type diffusion leads to an oscillation of the fluidities (e.g. Fig. 2a). In order to obtain an oscillating behaviour also for λ_A-type diffusion, λ_A is to be controlled by the degree of alignment, α_P. That is, starting with $\lambda_A = 0$, then if α_P exceeds a threshold value, the setting $\lambda_A \neq 0$ leads to a weakening of the actual alignment until α_P falls below a certain value affecting $\lambda_A = 0$, so that the process may start again (e.g. Fig. 2b).

6. SUMMARY

The pure mechanical part of the model is essentially controlled by two parameters, α and β. Correspondingly, three variations of the evolution equation are considered: (A) $\alpha = 0, \beta = 0$ (single slip); (B) $\alpha \neq 0, \beta = 0$ (grain interaction); (C) $\alpha = 0, \beta \neq 0$ (double slip). For model A it can be shown that under simple shear deformation the ODF develops a single maximum along the maximum eigenvalue of $\mathbf{D}$. As a result, the material reflects hardening behaviour in contradiction to experimental evidence. On the other hand, assuming deformation path independency, it was shown that the structure tensor may be identified with the Cauchy–Green tensor $\mathbf{B}$. This corresponds to the ideas published by Morland and Staroszczyk (1998) and Staroszczyk and Morland (2001). As was shown in earlier work, the interaction parameter α (model B) is active solely for the strain field within a grain, i.e. it vanishes via homogenization. Consequently, the stress relations for models A and B are macroscopically identical. Figures 1 and 2 show that the model is capable of reproducing essential features at least qualitatively. That is, one may observe an increasing shear fluidity due to an increasing c-axes alignment perpendicular to the shear direction. However, comparison with experiments (Budd and Jacka, 1989; Jacka and Li, 2000) reveals that softening induced solely by the texture development does not meet quantitative requirements, so an additional softening (enhancement factor) must be considered.

Originally motivated by the need for a numerically more efficient theory, especially if one is concerned with fully three-dimensional problems, the proposed constitutive equations represent a combination of a classical approach based essentially on representation theorems and an ODF-based mesoscopic theory. The implementation of the proposed structure tensor-based model into a fully coupled finite-element scheme will be discussed elsewhere.

REFERENCES

Advani, S. G. and C. L. Tucker. 1987. The use of tensors to describe and predict fiber orientation in short fiber composites. *J. Rheology*, **31**(8), 751–784.

https://doi.org/10.3189/172756403781815375 Published online by Cambridge University Press

Bouchez, J. L. and P. Duval. 1982. The fabric of polycrystalline ice deformed in simple shear: experiments in torsion, natural deformation and geometrical interpretation. *Textures and Microstructures*, **5**, 171–190.

Budd, W. F. and T. H. Jacka. 1989. A review of ice rheology for ice sheet modelling. *Cold Reg. Sci. Technol.*, **16**(2), 107–144.

Castelnau, O., Th. Thorsteinsson, J. Kipfstuhl, P. Duval and G.R. Canova. 1996. Modelling fabric development along the GRIP ice core, central Greenland. *Ann. Glaciol.*, **23**, 194–201.

Dafalias, Y. F. 1984. The plastic spin concept and a simple illustration of its role in finite plastic transformations. *Mech. Mater.*, **3**, 223–233.

Gagliardini, O. and J. Meyssonnier. 1999. Plane flow of an ice sheet exhibiting strain-induced anisotropy. *In* Hutter, K., Y. Wang and H. Beer, *eds. Advances in cold-region thermal engineering and sciences: technological, environmental, and climatological impact.* Berlin, etc., Springer-Verlag, 171–182. (Lecture Notes in Physics 533.)

Gödert, G. 1999. A meso–macro model for the description of induced anisotropy of natural ice, including grain interaction. *In* Hutter, K., Y. Wang and H. Beer, *eds. Advances in cold-region thermal engineering and sciences: technological, environmental, and climatological impact.* Berlin, etc., Springer-Verlag, 183–196. (Lecture Notes in Physics 533.)

Gödert, G. and K. Hutter. 2000. Material update procedure for planar transient flow of ice with evolving anisotropy. *Ann. Glaciol.*, **30**, 107–114.

Jacka, T. H. and Li Jun. 2000. Flow rates and crystal orientation fabrics in compression of polycrystalline ice at low temperatures and stresses. *In* Hondoh, T., *ed. Physics of ice core records*. Sapporo, Hokkaido University Press, 83–102.

Montagnat, M. and P. Duval. 2000. Rate controlling processes in the creep of polar ice: influence of grain boundary migration associated with recrystallization. *Earth Planet. Sci. Lett.*, **183**(1–2), 179–186.

Morland, L. and R. Staroszczyk. 1998. Viscous response of polar ice with evolving fabric. *Continuum Mech. Thermodyn.*, **10**(3), 135–152.

Poirier, J.-P. 1985. *Creep of crystals.* Cambridge, etc., Cambridge University Press.

Staroszczyk, R. and L.W. Morland. 2001. Strengthening and weakening of induced anisotropy in polar ice. *Proc. R. Soc. London, Ser. A*, **457**(2014), 2419–2440.

Thorsteinsson, Th., J. Kipfstuhl and H. Miller. 1997. Textures and fabrics in the GRIP ice core. *J. Geophys. Res.*, **102**(C12), 26,583–26,599.

Van der Veen, C. J. and I. M. Whillans. 1994. Development of fabric in ice. *Cold Reg. Sci. Technol.*, **22**(2), 171–195.

APPENDIX A

$$\int_{S^d} \nabla_{\mathbf{n}} \circ \Phi \, \mathrm{d}S^d = \mathrm{d} \int_{S^d} \mathbf{n} \circ \Phi \, \mathrm{d}S^d \,,$$
$$\int_{S^d} f(\cdot) \nabla_{\mathbf{n}} \otimes \mathbf{n} \, \mathrm{d}S^d = \mathbf{I} - \mathbf{A} \qquad \text{(A1)}$$

Here, $\circ \in \{\cdot, \times, \otimes\}$ is used as a general product operator.

APPENDIX B

$$\begin{aligned}
\langle f^{-1} \nabla_{\mathbf{n}} \cdot \mathbf{q}_{v_n} \mathbf{N} \rangle &= -2 \operatorname{sym}(\langle f^{-1} \mathbf{q}_{v_n} \otimes \mathbf{n} \rangle) \\
\nabla_{\mathbf{n}} I_{\mathbf{NX}^i} \otimes \mathbf{n} &= \mathbf{X}^i \cdot\cdot (\mathbf{N} \otimes \nabla_n) \otimes \mathbf{n} \\
&= \mathbf{X}^i \cdot\cdot \\
&\quad [\mathbf{n} \otimes (\mathbf{n} \otimes \nabla_n) \otimes \mathbf{n} + \mathbf{n} \otimes (\mathbf{n} \otimes \nabla_n) \otimes \mathbf{n}] \\
&= 2[\mathbf{X}^i \mathbf{N} - (\mathbf{N} \cdot\cdot \mathbf{X}^i) \mathbf{N}]
\end{aligned}$$

$$\nabla_{\mathbf{n}} I_{\mathbf{NX}^i} \otimes \mathbf{n} + \mathbf{n} \otimes \nabla_{\mathbf{n}} I_{\mathbf{NX}^i} = 2[\mathbf{N}\mathbf{X}^i + \mathbf{X}^i \mathbf{N} - 2\mathcal{N} \cdot\cdot \mathbf{X}^i]$$
$$2 \operatorname{sym}(\mathbf{q}_{v_{\mathbf{n}}} \otimes \mathbf{n}) = -4 f(\mathbf{n}, \mathbf{x}, t) \lambda_{\mathbf{a}} \mathcal{P}_{\mathbf{n}} \cdot\cdot \sum_{(i)} \mathbf{X}^i (3 - i) h_i I^{2-i}_{\mathbf{NX}^i} \,.$$

APPENDIX C

First-order tensors (vectors) are denoted by small letters, $\mathbf{t}$, and second-order tensors by capital letters $\mathbf{T}$. Tensors of arbitrary order are given through $\overset{\langle \mathrm{n} \rangle}{\mathbf{T}} = T_{i_1,i_2,\ldots,i_n} \mathbf{e}_{i_1} \otimes \mathbf{e}_{i_2} \otimes \ldots \mathbf{e}_{i_n}$, where $\overset{\langle \mathrm{k} \rangle}{\mathbf{A}} \otimes \overset{\langle 1 \rangle}{\mathbf{B}} A_{i_1,i_2,\ldots,i_k} B_{j_1,j_2,\ldots,j_l} \mathbf{e}_{i_1} \otimes \mathbf{e}_{i_2} \otimes \ldots \mathbf{e}_{j_l}$ represents the tensor product. Transposition is given through $\overset{\langle \mathrm{n} \rangle}{\mathbf{T}}{}^T = T_{i_n,i_{n-1},\ldots,i_1} \mathbf{e}_{i_1} \otimes \mathbf{e}_{i_2} \otimes \ldots \mathbf{e}_{i_n}$. The inner product of tensors of equal order is defined via contraction $\overset{\langle \mathrm{k} \rangle}{\mathbf{A}} \underbrace{\cdot\cdot\cdot}_{k} \overset{\langle \mathrm{k} \rangle}{\mathbf{B}}{}^T = A_{i_1,i_2,\ldots,i_n} B_{i_1,i_2,\ldots,i_n}$, so an inner product of two second-order tensors is given by their two-fold contraction $(\mathbf{A}, \mathbf{B}) = \mathbf{A} \cdot\cdot \mathbf{B}^T$, also compactly written as the first invariant $I_{\mathbf{AB}}$ of the tensor $\mathbf{A} \cdot \mathbf{B}$. Second-order tensors may be uniquely decomposed into a symmetric, $\operatorname{sym}[\mathbf{A}] = \frac{1}{2}(\mathbf{A} + \mathbf{A}^T)$ and an asymmetric part, $\operatorname{skw}[\mathbf{A}] = \frac{1}{2}(\mathbf{A} - \mathbf{A}^T)$. Anticipating further the need for generalized higher-order orientation tensors, the recursive formula for the mesoscopic structure tensors, $\overset{\langle \mathrm{k} \rangle}{\mathbf{N}} = \overset{\langle \mathrm{k}-1 \rangle}{\mathbf{N}} \otimes \overset{\langle 1 \rangle}{\mathbf{N}}$, where $\overset{\langle 1 \rangle}{\mathbf{N}} = \mathbf{n}$, is to be established, where $\mathbf{n} = \sin\Theta \, \cos\varphi \mathbf{e}_1 + \sin\Theta \sin\varphi \mathbf{e}_2 + \cos\Theta \mathbf{e}_3$. Alternative notation of fourth-order tensors is given as $\mathcal{N} = \overset{\langle 4 \rangle}{\mathbf{N}}$, $\mathcal{I}_{\mathrm{sym}} = \frac{1}{2}(\delta_{ik}\delta_{jl} + \delta_{il}\delta_{jk})$ and $\mathcal{I}_{\mathrm{dev}} = \mathcal{I}_{\mathrm{sym}} - \mathbf{I} \otimes \mathbf{I}$, representing the fourth-order structure tensor, the identities on the space of symmetric and symmetric deviatoric tensors, respectively.

https://doi.org/10.3189/172756403781815375 Published online by Cambridge University Press